Asian J. Adv. Basic Sci.: **2015, *4(1)*,** 12-24
ISSN (Print): 2454 – 7492
ISSN (Online): 2347 – 4114
www.ajabs.org

Preparation and Characterization of *Polyalthia longifolia* Based Alumina as a Novel Adsorbent for Removing Fluoride from Drinking Water

Sanghranta S. Waghmare[1*], Tanvir Arfin[1], Nilesh Manwar[1], Dilip H. Lataye[2], Nitin Labhsetwar[1] & Sadhana Rayalu[1]

[1& *] *Environmental Materials Division, CSIR-National Environmental Engineering Research Institute (CSIR-NEERI), Nagpur, INDIA*
[2] *Civil Engineering Department, Visvesvaraya National Institute of Technology, Nagpur, INDIA*
[*] *Correspondance: E-mail: ss_waghmare@neeri.res*

(Received 17 Aug 2015; Accepted 18 Aug, 2015; Published 20 Aug, 2015)

ABSTRACT: This research addresses i) synthesis of an alumina composite based on high capacity adsorbent using a leaf as a template and ii) the issue of handling spent regenerant resulting from regeneration of such high capacity adsorbents. A low-cost composite type adsorbent has been synthesized for removal of excess fluoride from drinking water, using *Polyalthia longifolia* (false Ashoka tree) leaf as a template and alum as a source of alumina. The composite adsorbent having heterogeneous phases of $Al(OH)_3$ and Al_2O_3 is associated with carbon and free $Al(OH)_3$ and alumina has been identified using XRD, SEM, FTIR and BET surface area analysis. Batch adsorption experiments were carried out including the effect of various physico-chemical parameters, such as adsorbent dose, pH, contact time, initial fluoride ion concentration and temperature to ascertain optimal performance conditions. The elemental composition of material and SEM analysis suggests a composite material with different phases. *Polyalthia longifolia based adsorbent* (PBA) effectively removes fluoride with substantially high adsorption capacity of 17.57 mg g^{-1} at initial fluoride concentration of 5 mg l^{-1} using very low dose of 0.4 g l^{-1} as compared to 1.82 mg g^{-1} for activated alumina. PBA has been regenerated to the tune of about 80% using alum solution. The spent regenerant has been subjected to two new options i) recovery of alum and formation of chitosan/CaF composite by treating with slaked lime and ii) immobilization of AlF in chitosan to form chitosan/AlF composite. These composites may prove to be useful optic materials for UV absorption.

Keywords: Adsorbent; adsorption; entropy; enthalpy and kinetics**.**

INTRODUCTION: Fluoride is recognized as one of the chief pollutants in drinking water in several parts of the globe. Fluoride uptake is helpful to the human body when its intake is inside of as far as possible. It is essentially required for calcification of dental enamel and maintenance of healthy bones. The presence of excessive fluoride beyond prescribed limit of 1.5 mg l^{-1} affects the metabolism of Ca, P, etc. in the human body and causes permanent bones joint deformation and fluorosis.[1] Skeletal and dental fluorosis are permanent damages with generally no remedial treatment. The only preventive measure is to reduce the intake of fluoride. The stipulated limit of fluoride in water is 1.5 mg l^{-1} (WHO) while 1.0 mg l^{-1} (Indian BIS standards), and therefore it is imperative to remove excess fluoride from water.

An widespread range of technologies has been employed for fluoride treatment from water including flotation, precipitation, coagulation, oxidation, solvent extraction, evaporation, distillation, reverse osmosis, ion exchange, electrodialysis, electrolysis, adsorption, etc.[2,3&4] All these procedures have significant limitations, which are for instance, incomplete fluoride removal, high-energy requirements, and generation of toxic sludge or waste products that also require disposal.[5] Adsorption is considered as one of the suitable water treatment methods due to its ease of operation, which is dependent on ions (adsorbate) in fluid diffusing to the surface of a solid (adsorbent), where they bond with the solid surface or are held there because of weak intermolecular forces.[6] Among all of the defluoridation adsorbents, alumina based and carbonaceous materials such as activated carbon[7] and carbon nanotubes[8] are the most commonly used adsorbents due to their large specific surface area, large quantity of surface functional groups, and adequate pore size distribution. The utilization of characteristic natural biomaterials is a promising option due to their relative abundance and their low commercial value. *Polyalthia longifolia* (false Ashoka tree) is the most ancient tree native to India and Sri Lanka belonging to family Annonaceae. This type of indigenous tree is found throughout India, especially in Himalaya, Kerala, Bengal and whole of the south region. Aerial of the tree have significant anti-inflammatory activity and medicinal value.[9] *Saracaasoca* (Ashoka tree) leaves were used as adsorbent for removal of dyes.[10] In this study, the fluoride adsorption properties of synthesized *Polyalthia longifolia* (false Ashoka tree) leaf based alumina (PBA) composite adsorbent were studied through detailed batch adsorption study, including effect of PBA dose, initial fluoride concentration, pH, contact time, and co-anions study. Adsorption isotherm, kinetic models and thermodynamic parameters have also been estimated from experimental results. The issue of handling powered sample has been addressed by immobilizing it in biopolymer. The issue of handling spent regenerate has been handled by immobilizing CaF/AlF in polymer.

MATERIAL AND METHODS: All chemicals used in the present study were of analytical reagent grade. Sodium fluoride, sodium chloride, sodium sulfate, sodium nitrate, sodium bicarbonate and sodium carbonate were obtained from E-Merck India Ltd., Mumbai, India. A stock solution of fluoride was prepared by dissolving 2.21g sodium fluoride in 1L of de-ionized water, and test fluoride solution of 5mg L^{-1} was prepared from fresh stock fluoride solution by appropriate dilution.

Synthesis of Adsorbent: *Polyalthia longifolia* (false Ashoka tree) based alumina (PBA) composite adsorbent was prepared using false Ashoka tree leaf powder and aluminium sulfate. The PBA synthesis was carried by optimizing various synthesis conditions for egg shell composite materials.[11] The conditions such as aluminium quantity, shaking time, calcination temperature and duration have a significant effect on the synthesis of PBA. These conditions were optimized by varying the parameters within feasible parametric range. Synthesized adsorbents were evaluated for fluoride removal to optimize the best condition for PBA synthesis and thus adsorption capacity was considered as the important criteria for optimizing synthesis. The synthesis protocol of PBA is provided below:

5.56 g of aluminium sulfate (reagent grade) was dissolved in 25 mL of distilled water. *Polyalthia longifolia* (false Ashoka tree) leaf powder (3 g) was added into aluminium sulfate solution. The above mixture was stirred on a horizontal shaker for 4hrs. This mixture was transferred to an evaporating dish and dried at 110°C in a muffle furnace for 3 hrs followed by calcination at 450°C for 6 hrs. The calcined material was then grounded in a mortar pestle and washed with distilled water in 1:20 (material: distilled water) ratio by shaking on horizontal shaker for 24 h followed by 1 h more washing. Finally, material was dried at 70ºC in oven for 4 h.

Batch Adsorption Study: The adsorption studies for fluoride removal from drinking water by PBA were carried out in a batch process. 50mL of the test fluoride solution was taken into a 250mL of PVC conical flask and known weight of adsorbent was added to it and then shaken at 150 rpm on a horizontal rotary shaker (Model No.CIS-24, Remi Instruments, Mumbai, India) for 24 h in order to attain equilibrium. The flask was removed from the shaker and then allowed to stand for 5 min for settling the adsorbent. The solution was then filtered using Whatman filter paper No. 42 and the filtrate were analyzed for residual fluoride concentration using selective ion electrode. The total ionic strength adjusting buffer (TISAB-III) was added in 1:10 (mL) ratio to the sample and standard solutions to regulate the ionic strength. The addition of TISAB also resulted in pH adjustment and elimination of polyvalent cations such as Al (III), Fe(III) and Si(IV). These polyvalent cations have the ability to form the complex or precipitate with the fluoride ions and reduce the free fluoride concentration in the solution. Similarly, all the fluoride removal experiments were studied at different operational conditions including the effect of adsorbent dose, initial fluoride concentration, solution pH and effect of co-ion on fluoride removal. All the experiments were carried out at room temperature (25ºC± 2ºC).The specific amount of fluoride adsorbed was calculated using following Eq. (1)

$$q_e = (C_0 - C_e)\frac{V}{m} \qquad (1)$$

where q_e is the adsorption capacity (mg g^{-1}) in the solid at equilibrium; C_0 and C_e are initial and equilibrium concentrations of fluoride (mg L^{-1}) respectively; *V* is volume of the aqueous solution and *m* is the mass (g) of adsorbent used in the experiments. The effect of pH on fluoride removal was studied by adjusting the pH of the solution using 0.1N HCl and 0.1N NaOH. Adsorption kinetic study was carried out by adding 0.02 g of PBA into 250mL of PVC conical flask 50 mL solution with different fluoride concentrations (5, 10 and 15 mg l^{-1}) to determine the minimum time required for adsorption to reach equilibrium at pH=7.0 and at temperature of (293,303, and 323 K). The amount of adsorption at time t, q_t (mg g^{-1}) was calculated by:

$$q_t = (C_0 - C_t)\frac{V}{m} \qquad (2)$$

where C_t (mg l^{-1}) is the concentration of fluoride ions at indicated time.

Thermodynamic parameters of adsorption standard Gibb's free energy change ($\Delta G°$), standard enthalpy change ($\Delta H°$), and standard entropy change ($\Delta S°$) were calculated at 293, 303, and 323 K.

Method of Analysis: The fluoride concentration in the treated water sample was measured using selective ion electrode 9609 BNWP Orion (USA make) attached with Orion 920A+ ISE/pH/mV/ORP meter. Similar ion meter coupled with pH electrode was used for measuring pH of the treated samples. The leaching of metals from the adsorbent was determined using Inductively Coupled Plasma-atomic emission spectroscopy (ICP-AES, Model OPTIMA 4100DV). Experiments were repeated twice with better accuracy, and blank experiments were also performed throughout the studies. The similar experimental procedure was followed to study the effect of co-existing ions, pH and initial concentration of fluoride, etc. for adsorption of fluoride on PBA material. Water quality parameters of the treated and untreated water samples were analysed using standard methods.[1]

Physical Characterization: XRD patterns of PBA as such and after treatment with fluoride were recorded on Rigaku Mini flex II, Desktop X- Ray diffractometer with CuKα radiation (λ 0.5405), in order to study the structural changes if any. The sample was scanned for 2θ range from 10° to 80°. The FTIR spectra of PBA (before and after fluoride adsorption) in KBr pellets were recorded on a Bruker Model Vertex 70 spectrometer. The surface morphology of the PBA as such and after treatment with fluoride ion was determined by using Scanning Electron Microscope (Jeol, JXA-840 A) coupled with Electron probe micro-analyser. The surface area of PBA was measured by Brauner, Emmett and Teller (BET) method using Micro-meritics ASAP2010 surface area analyser.

RESULTS AND DISCUSSION:

Characterization of PBA adsorbent:

XRD patterns of PBA adsorbent: All the materials produce the diffraction patterns on interacting with the X-ray source. XRD, a significant process for the crystalline studies is being used in the method of Crystallography.[12] Exertion has been made to elucidate structural details and phase identification of PBA composite adsorbent using XRD analysis. Figure1 shows the XRD patterns of PBA (a) before fluoride adsorption and (b) after fluoride adsorption.The basic refinement of XRD data has been performed , and efforts were made for phase identification. The XRD analysis shows the presence of multiple phases with a prominent presence of crystalline alumina phases as well as some amorphous phases. The XRD pattern of fluoride adsorbed PBA shows the formation of Aluminium fluoride complexes. Based on the XRD analysis, it was observed that the crystal structure of PBA showed no significant change after fluoride adsorption, thereby inferring its stable nature. The repeat synthesis of this material shows excellent reproducibility, which is important in the case of such a composite type material.[13]

SEM morphology of PBA adsorbent: Scanning Electron Microscopy of PBA adsorbent is helpful in understanding its surface structure.[14] Figure 2 (a) and (b) shows the SEM images of PBA before fluoride and after fluoride adsorption respectively. The SEM image of PBA as such suggests the presence of both coarse and fine particles with irregularly shaped particles of alumina with agglomerates of small particles adhered on carbon particles. The SEM of PBA after fluoride treatment also shows both coarse and fine particles with irregularly shaped particles of alumina. Table 1 shows the approximate chemical analysis results for the Ashoka leaf based composite adsorbent media. The chemical compositions of the material indicate that it is a composite material consisting of different phases. These findings also infer that alumina based phases are the major components of this material while the presence of significant amount of carbon suggests the possibility of its presence as support or incorporation in the alumina phase.

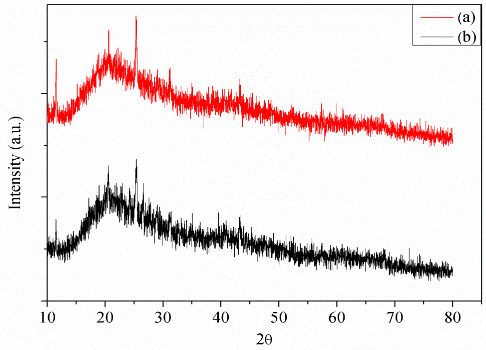

Figure 1: XRD patterns of PBA a) before fluoride adsorption b) after fluoride adsorption.

Table 1: Chemical analysis results for PBA.

Parameter	%
C	2.77
H	3.57
N	0.38
S	7.15
Aluminium as Al	7.92

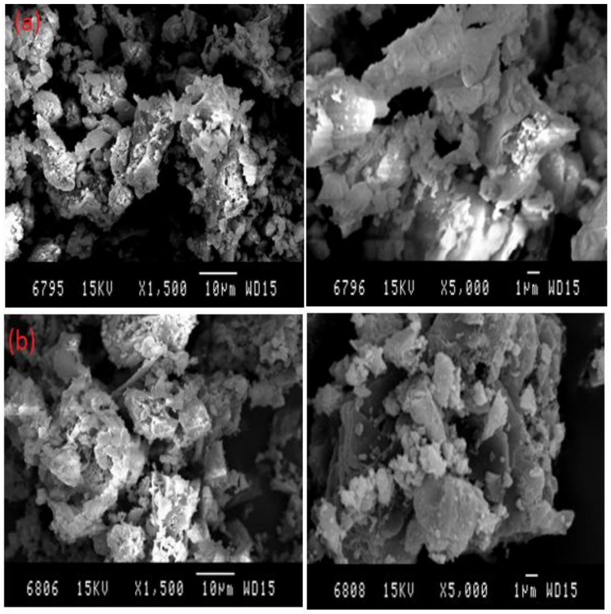

Figure 2: SEM morphology of PBA a) before fluoride adsorption b) after fluoride adsorption.

BET analysis of PBA adsorbent: The adsorbent's physical property is crucial and significantly influences adsorption capacity. The specific surface area of the PBA was carried out after fluoride adsorption, and the result shows the value of 19.71 m^2g^{-1}.

FTIR studies of PBA adsorbent: Infrared spectra were listed in the range of 4000-600 cm^{-1} using a normal resolution of 8 cm^{-1} and 32 scans per spectrum. The FTIR spectra of PBA adsorbent before and after adsorption of fluoride are shown in Figure 3. The peak at **3614 cm^{-1}** can be assigned to the broad adsorption peak of –OH group, while the peak at **1678 cm^{-1}** represents stretching vibration of C=O group.[15] The peak observed at **1423** and **1361 cm^{-1}** can be assigned to the vibration of –OH group of the primary alcoholic group and CO-NH group of amide respectively. The intense peak appeared at **1129 cm^{-1}** corresponds to the vibration of $–SO_4$ groups. The peaks at **716** and **670 cm^{-1}** can be attributed to Al-O stretching mode and O-Al-O bending mode respectively.[16]

Two absorption peaks were observed at **3675 and 1616 cm^{-1}** which correspond to the primary amine ($–NH_2$) in after adsorption of fluoride, which may be due to H-bonding between the protonated amine and the fluoride. The increase in the intensity of bands at **1690 cm^{-1}** and **1514 cm^{-1}** in after adsorption of fluoride was observed, which may be due to the exchange of fluoride with –OH group of primary hydroxyl group, and the interaction of fluoride with metal ions i.e. Al^{+3}. The loss of intensity of the peak at **678 cm^{-1}** (O-Al-O bending mode) was observed, which suggest the interaction of fluoride with metal ion i.e., Al^{+3}.

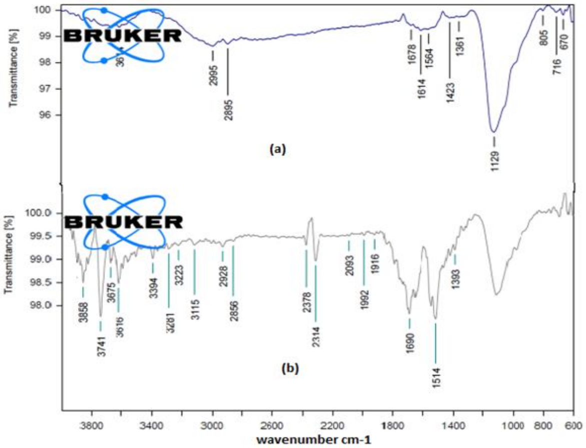

Figure 3: FTIR spectra of PBA a) before fluoride adsorption b) after fluoride adsorption.

The schematic mechanism: The heterogeneous sample of Al(NP) deposited and encapsulated with carbon in addition to water forms $Al(OH)_3$ by the following reaction scheme that could describe the major mechanism of fluoride removal.

$$Al + 3H_2O \longrightarrow Al(OH)_3 + 3H_2\uparrow$$

$$2Al + 3H_2O \longrightarrow Al_2O_3 + 3H_2\uparrow$$

The $Al(OH)_3$ so formed is amorphous in nature and appears to have a high affinity for fluoride. Besides, the composite of carbon and $Al(OH)_3$; the PBA sample is also expected to have separate $Al(OH)_3$ and carbon phases as well.

As illustrated in Scheme-I, the synthesis entails four steps, the details of which are as follows:

Step-I: The first step is mixing of biomaterial (leaves) with alum solution, which leads primarily to following two reactions:

- Reduction of Al^{3+} to Al(NP) with reducing and capping agent like extracellular protein / polysaccharide (EPs) and sesquiterpene derivatives associated with leaves.
- Adsorption of Al^{3+} on negatively charged a functional group of the cell membrane.

Step-II: Involves heating at 110 ^oC to ensure improvement in adsorption of Al^{3+}. At low pH of the slurry (leaf + alum), the surface charge of the cell is positive with consequent decrease in binding of (positive) metal ions, however thermal heating at 110^0C probably generates additional binding sites via denaturation of protein on the cell wall structure, thus improving metal adherence to cell wall structure of leaves.

Step-III: In this step the thickened slurry is subjected to carbonisation wherein the Al^{3+} encapsulated with protein and the Al^{3+} deposited on cell wall structure are both reduced to Al(NP) as core shell structure in the first case and Al(NP) deposited on carbon in the second case.

Step -IV: Involves washing with water to remove the excess unreacted aluminium ions. In addition to the Al(NP) deposited and encapsulated on carbon, the Al(NP) and carbon also exists as separate phases. Studies are now in progress for breakup synthesis to identify the phase showing a maximum of fluoride removal.

Batch adsorption study:

Preliminary study: A preliminary adsorption experiment was carried out using false Ashoka tree leaf powder (as reference) and PBA at initial fluoride concentration 5.3 mg l^{-1} and contact time of 18 h, to check the fluoride removal efficiency of both adsorbents, as shown in Figure 4. The PBA shows much higher fluoride removal efficiency compared to false Ashoka tree leaf powder. Therefore further adsorption studies for fluoride removal were carried using PBA.

Effect of adsorbent dose: The effects of adsorbent dose on fluoride removal using PBA was investigated at fixed initial fluoride concentration of 5.3 mg l^{-1}, pH = 7.43, shaking speed of 150 rpm, and contact time of 18 h, as shown in Figure 5. It was noticed that percent removal of fluoride evidently increases from 66.67% to 96.97%, while the equilibrium fluoride adsorption capacity decreases from 22 mg/g to 8.0 mg/g with the increase in adsorbent dose of PBA from 0.02 to 0.08 g/100ml. This is due to the higher active site: fluoride ratio. However, no significant change in the fluoride removal was observed after a dose of 0.04 g/100ml, which might be due to the lower equilibrium fluoride ion concentration per the active site of the adsorbent for adsorption. Fluoride concentration of 0.20 mg l^{-1} was achieved at a dose of 0.8 g l^{-1}, which is as well below the permissible limit of 1.5 mg l^{-1} for drinking water. Also, no leaching of the aluminum ion was observed at a dose of 0.04 g/100ml. Therefore, an adsorbent dose of 0.4 g l^{-1} was considered as optimum for further fluoride removal studies.

Effect of initial fluoride concentration: The effect of initial fluoride concentration on fluoride adsorption by PBA was studied at different initial fluoride concentrations by keeping all other parameters constant (PBA dose 0.4 g l^{-1}, temperature $25^{0}C \pm 2\ ^{0}C$, shaking speed 150 rpm, contact time 18 h and pH 7.40) as shown in Figure 6. This was observed that with an increase in fluoride concentration, percent fluoride removal decreases, while fluoride adsorption capacity increases. This should be due to the more availability of fluoride ions at higher fluoride concentration for adsorption. A closer look of these results infer that the increase in adsorption capacity (qe) is more significant than the decrease in percent fluoride removal as much as more than 69.50 mg g^{-1} of qe could be achieved at higher concentration, which is relatively very high when compared with reported adsorbents.

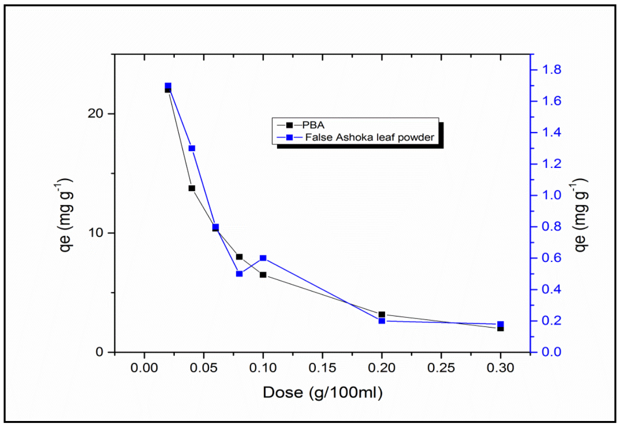

Figure 4: Comparison of fluoride removal efficiency of PBA and False Ashoka tree leaf powder.

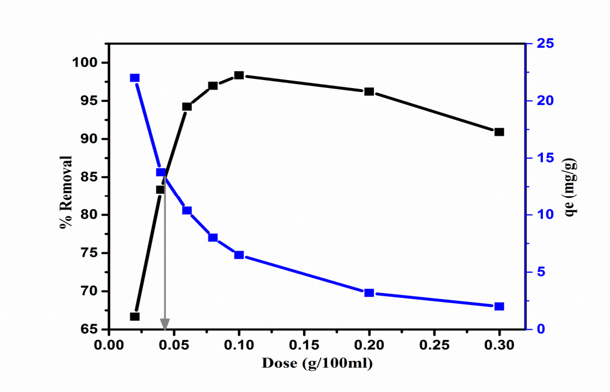

Figure 5: Effect of adsorbent dose on fluoride removal using PBA.

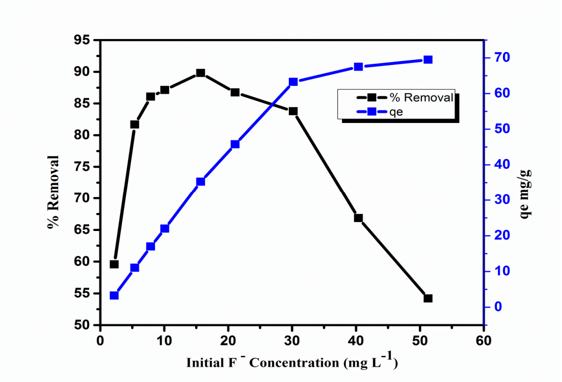

Figure 6: Effect of initial Concentration (C_0) on fluoride removal using PBA.

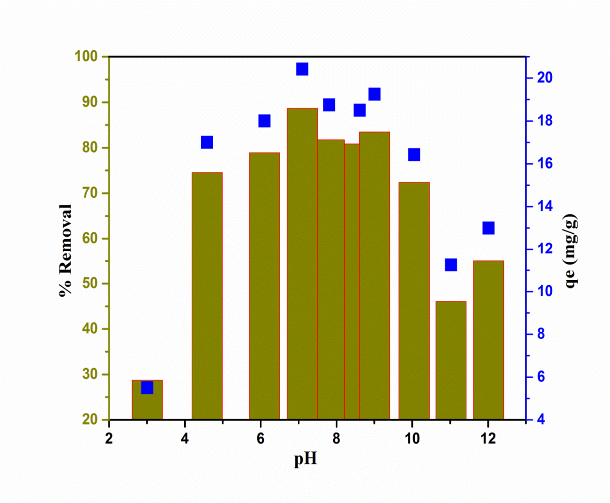

Figure 7: Effect of pH on fluoride removal using PBA.

Effect of pH: The effect of pH on fluoride removal by PBA was studied by varying solution pH from 3 to 12, with Initial fluoride concentration = 5.3 mg l^{-1}; adsorbent dose = 0.4g l^{-1}; contact time = 18h; shaking speed = 150 rpm and temperature = 25±1°C. The results thus obtained are presented in Figure 7. It appears that there was no significant effect on the fluoride removal over a wide range of pH 5-10, which is quite advantageous considering the low pH requirements for some of the commonly used activated alumina based adsorbents. Hence, present adsorption process is independent of pH change. However, the decrease in fluoride removal was observed at highly acidic (pH < 4) and alkaline (pH > 10) medium, which are of no practical significance for drinking water treatments methods. This decreased fluoride removal in highly acidic condition may be attributed to the fact, that at pH below 5, formation of weakly ionized hydrofluoric acid takes place,[17] whereas, at highly alkaline condition (above pH 10), negatively charged hydroxyl ions compete with fluoride ions on adsorbent surface. Maximum fluoride adsorption was observed for water (Tap water) of pH= 7.51. While in acidic and alkaline pH fluoride removal slightly decreases. However, at neutral pH which is normally pH of drinking water, the concentration of aluminium is within the permissible limit of 0.2 mg l^{-1}. Hence, PBA can be used for defluoridation of drinking water.

Effect of co-existing anions: Fluoride contaminated ground water contains several other anions such as sulphate chloride, nitrate, bicarbonate, carbonate which compete with fluoride in adsorption process due to their similar negative charge. The sodium salt of sulphate, chloride, nitrate, carbonate and bicarbonate were used for this study. Fluoride adsorption studies with the influence of these interfering ions were carried out at different concentrations of co-anions from 100 mgl^{-1} to 600 mgl^{-1}. The effect of co-existing ions on fluoride removal is shown in Figure 8. The order of anions influencing the fluoride removal efficiency was observed as CO_3^- >HCO_3^-> SO_4^{2-}> NO_3^->Cl^-. It is observed that the presence of chloride, sulphate and nitrate ions has a negligible effect on fluoride removal by PBA. It is observed that in presence CO_3^- and HCO_3^- the pH of the fluoride solution was alkaline (10.8) and fluoride adsorption capacity decrease at pH 11 as shown in Figure 4. Therefore, fluoride removal efficiency decreases drastically with increase in $CO_3^-$and HCO_3^- concentration above 300 mg^{-1}, however, such high concentrations of CO_3^- and HCO_3^- ions are not commonly found in ground water, while it is also noticeable that the fluoride removal even in presence of these competing ions was still quite high as compared to many adsorbents reported before.[18&19]

Adsorption Isotherm Study: The Langmuir adsorption model can be represented in linear form as follows:[20]

$$\frac{1}{q_e}=\frac{1}{q_{\max}K}\times\frac{1}{C_e}+\frac{1}{q_{\max}} \qquad (3)$$

where, q_{max} is the amount of adsorbate at complete monolayer coverage ($mg.g^{-1}$), which gives the maximum adsorption capacity of the adsorbent, K is the equilibrium constant of adsorbent at equilibrium which indicates the affinity of adsorbate toward adsorbent and q_e and C_e are the equilibrium adsorption capacity and equilibrium concentration of adsorbate in solution.

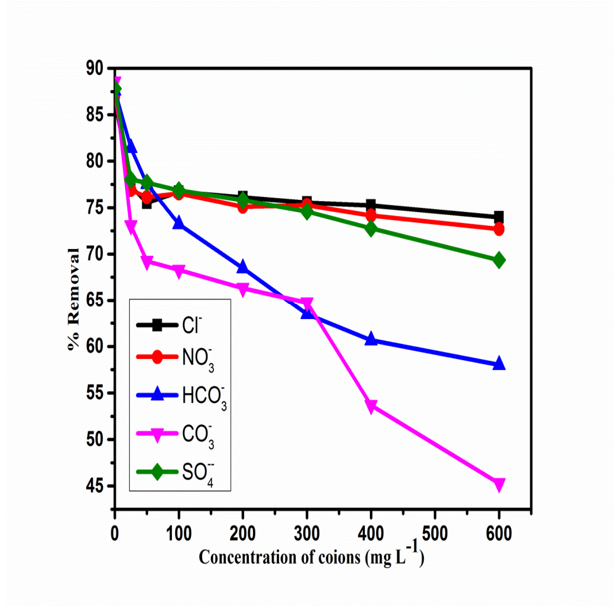

Figure 8: Effect of co-ions on fluoride removal efficiency using PBA.

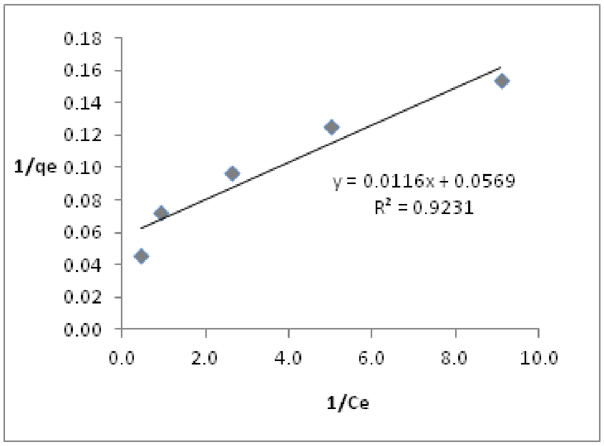

Figure 9: Linear model of Langmuir adsorption isotherm for fluoride removal using PBA.

In order to predict the feasibility of the isotherm, the essential characteristics of the Langmuir isotherm can be expressed in terms of a dimensionless constant separation factor (r) was calculated by using the following equation,[21]

$$r = \frac{1}{1 + KC_0} \qquad (4)$$

where, C_o and K are the initial concentration of adsorbate (mg l^{-1}) and Langmuir isotherm constant respectively.

The Freundlich model is given by the following linearized equation,[22]

$$\log(q_e) = \log K_F + 1/n \log(C_e) \qquad (5)$$

where K_F and 1/n are Freundlich constants related to adsorption capacity and adsorption intensity (heterogeneity factor) respectively.

The purpose of the adsorption isotherms is to reveal the specific relationship between the amount of adsorbate adsorbed and its equilibrium concentration in solution. In order to understand the adsorption of fluoride on PBA, the adsorbent dose was varied by keeping other parameters constant (PBA dose 0.2–3.0 g L^{-1}, $C_{0=}$ 6.6 mg L^{-1}, temperature 30 ^{0}C ± 2 ^{0}C, shaking speed 150rpm and contact time 18h). The experimental data were analysed using two important isotherms including Langmuir adsorption isotherm, which is valid for monolayer adsorption on the surface of adsorbent and Freundlich adsorption isotherm, which is indicative of the surface heterogeneity of adsorbent.

The values of q_{max} and K were calculated from the plot of $1/q_e$ vs. $1/C_e$ as shown in Figure 9. The r <1 indicate favourable adsorption and r >1 indicate unfavourable adsorption. The value of r for the initial concentration of 6.6 mg l^{-1} was found to be 0.0029. Thus, it indicates that the present system is favourable for adsorption of fluoride.

The values of K_F and 1/n were obtained from the slope and intercept of the linear Freundlich plot of log qe vs. log Ce as shown in Figure 10. The values of Langmuir and Freundlich constants are illustrated in Table 2.

The value of the adsorption intensity 1/n (heterogeneity factor) was observed between 0.1 and 1.0, which also indicates that the system is favourable for adsorption. The adsorption data can be successfully fitted to both Freundlich and Langmuir adsorption models, which is evident from the high R^2 value (0.976 and 0.923, respectively). Better fit of Freundlich isotherm model is indicative of the surface heterogeneity of adsorbent.

Table 2: The Langmuir and Freundlich adsorption constants for *Polyalthia longifolia* (false Ashoka tree) leaf based alumina (PBA) and activated alumina.

Adsorbents	Freundlich model			Langmuir Model		
	K_F (mg g^{-1})	1/n	R^2	q_{max} (mg g^{-1})	K (L mg^{-1})	R^2
PBA	3.232	0.766	0.976	**17.57**	51.72	0.923
A.A	-	-	-	1.82	0.28	0.96

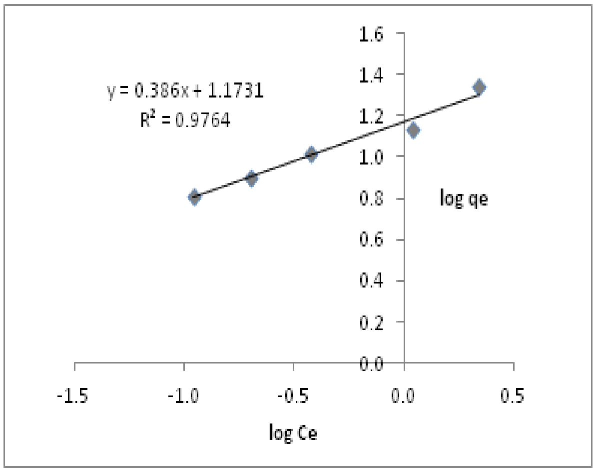

Figure 10: Linear model of Freundlich adsorption isotherm for fluoride removal using PBA.

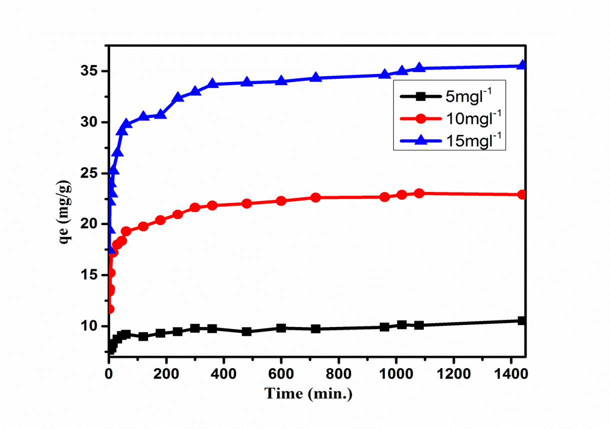

Figure 11: Effect of time on fluoride adsorption using PBA.

Adsorption kinetics: The pseudo-first-order equation of Lagergren is generally expressed as follows:[23]

$$\log(q_e - q) = \log q_e - \left(\frac{K_{ad}}{2.303}\right)t \qquad (6)$$

where, q_e and q (both in mg g^{-1}) are the amounts of fluoride adsorbed per unit mass of adsorbent at equilibrium and time (t) respectively, and K_{ad} is the rate constant (min^{-1}).

The pseudo second order model is also commonly used to predict the kinetic parameters linear form of which can be written as follows:[24]

$$\frac{t}{q_t} = \frac{1}{h} + \frac{t}{q_t} \qquad (7)$$

$$h = kq_e^2 \qquad (8)$$

where q_t is the amount of fluoride adsorbed at time t (mg g^{-1}), q_e is the amount of fluoride adsorbed at equilibrium (mg g^{-1}), h is the initial sorption rate (mg g^{-1} min^{-1}).

The rate constant for intra-particle diffusion was obtained by using the following equation:[25]

$$q = K_p \times t^{1/2} \qquad (9)$$

where K_p (mg g^{-1} $min^{-1/2}$) is the intra-particle diffusion rate constant.

Adsorption kinetic deals with the rate at which sorption occurs, where the rate is defined as the change of a given quantity over a specific period. The rate of fluoride adsorption on PBA was determined by studying the adsorption kinetics at different initial concentrations of 5.4, 10.3, 15.4 mg L^{-1} at optimum dose. From Figure 11, it was observed that fluoride uptake was very rapid in the first 10 min, and then the rate slowed down as the equilibrium was reached. The results obtained from the experiments were used to determine the rate-limiting step. Kinetic models are used to examine the rate of the adsorption process and potential rate-controlling step. The potential rate of PBA for fluoride removal following three different kinetic models: pseudo-first-order, pseudo-second-order and intra-particle diffusion was examined in this study.

The value of K_{ad} was calculated from the slope of the linear plot of log (qe-qt) vs. time as shown in Figure 12 (a). The adsorption rate constant was found to be 2.303× 10^{-03}, 2.303 × 10^{-03} and 3.454× 10^{-03} min^{-1} for initial fluoride concentration of 5.4, 10.3 and 15.4 mg l^{-1} respectively.

The values of qe, k and h can be calculated from the plots of t/qt vs. t and given in Table 3. The linear plots of the pseudo first-order (Eq. (6)) and pseudo-second-order (Eq. (8)) model represented in Figure 12(b). The variation in adsorption rate should be proportional to the first power of concentration for strict surface adsorption. However, the relationship between initial solute concentration and rate of adsorption will not be linear when pore diffusion limits the adsorption process. The possibility of a graphical relationship between the amount of fluoride adsorbed and the square root of time was investigated. The amount of fluoride sorbed per unit mass of adsorbents (q) at any time (t) was plotted as a function of square root of time, ($t^{1/2}$) in Figure 13 in order to show the existence of intra-particle diffusion in the adsorption process.

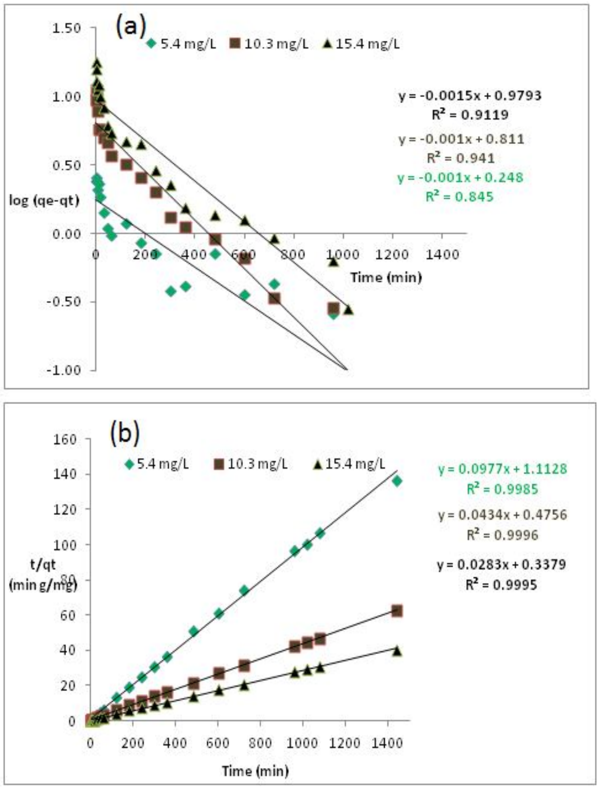

Figure 12: Adsorption kinetics :(a) Pseudo-First order, (b) pseudo-second order plot for fluoride removal using PBA.

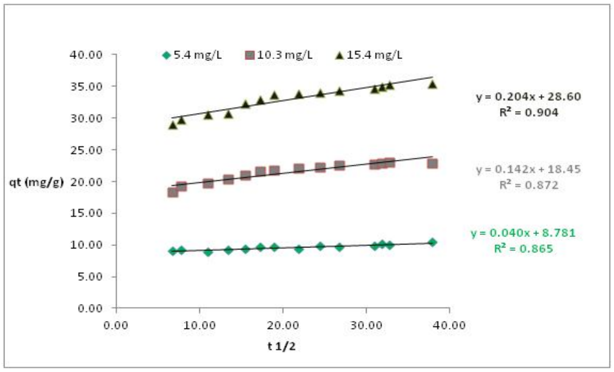

Figure 13: Intra-particle diffusion kinetic plot for fluoride removal using PBA.

The plot for intra-particle diffusion shows that initially curved portion reflects film or boundary layer diffusion effect and the subsequent linear portion are attributed to the intra-particle diffusion effect. The K_p values were obtained from the slope of the linear portion of the curves and were found to be 4.0 x 10^{-2}, 14.2 x 10^{-2} and 20.4 x 10^{-2} mg g^{-1} $min^{-1/2}$ at initial fluoride concentration of 5.4, 10.3 and 15.4 mg l^{-1} respectively. The linear portion of the curves does not pass through the origin indicating that the surface fluoride adsorption as well as intra-particles diffusion contributes to the rate determining step.

Table 3: Lagergren, Pseudo second order kinetic parameters, particle and intraparticle pore diffusion model parameter for different initial fluoride concentrations. (Volume: 500 ml, Temperature: 30±1°C, Adsorbent dose: 0.4 g/L).

C_o (mg l^{-1})	Lagergren parameters		Pseudo second order parameters			Particle Diffusion Model	
	K_{ad} (min^{-1})	R^2	k (g mg^{-1} min^{-1})	h (mg g^{-1} min^{-1})	R^2	k_p (mg g^{-1} $min^{-1/2}$)	R^2
5.4(~5)	2.303 x 10^{-3}	0.845	8.71x10^{-3}	0.8993	0.998	4.0 x 10^{-2}	0.865
10.3 (~10)	2.303 x 10^{-3}	0.941	3.99x10^{-3}	2.1053	0.999	14.2 x 10^{-2}	0.872
15.4(~15)	3.454 x 10^{-3}	0.911	2.39x10^{-3}	2.9674	0.999	20.4 x 10^{-2}	0.904

Thermodynamic parameters:To see the effect of temperature on the adsorption of fluoride by PBA, thermodynamic parameters associated with the adsorption process, viz. standard free energy change (ΔG°), standard enthalpy change (ΔH°) and standard entropy change (ΔS°) were calculated using the following equations.

The free energy of adsorption process is represented by the equation,[26]

$$\Delta G^\circ = -RT \ln Kc \qquad (10)$$

where, ΔG° is the free energy of sorption (KJ/mol), T is the temperature in Kelvin, R is the universal gas constant (8.314 $Jmol^{-1}K^{-1}$) and Kc is the sorption equilibrium constant.

The sorption equilibrium constant Kc may be expressed in terms of enthalpy change (ΔH°) and entropy change (ΔS°) as a function of temperature and is shown below.

$$\ln Kc = \frac{\Delta S^\circ}{R} - \frac{\Delta H^\circ}{RT} \qquad (11)$$

where ΔH° is the heat of sorption (KJ mol^{-1}) and ΔS° is the standard entropy change (KJ mol^{-1} K^{-1}).

The sorption equilibrium constant Kc for the sorption reaction was determined from the slope of the plot of ln(qe/Ce) Vs Ce at different temperatures and extrapolating to zero Ce.

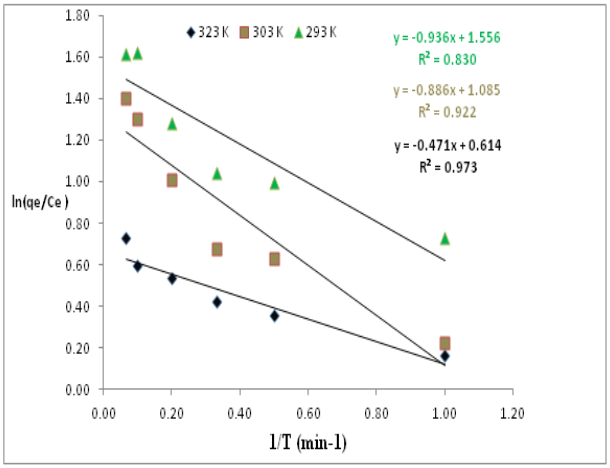

Figure 14: The plot of ln(qe/Ce) against 1/T for thermodynamic parameter for fluoride removal using PBA.

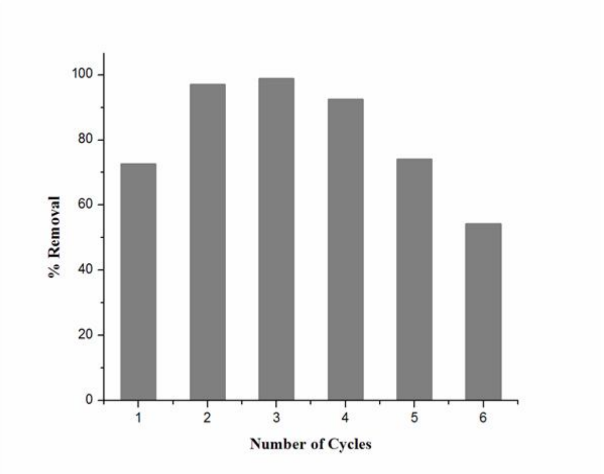

Figure 15: Reusability for fluoride removal using PBA.

Table 4: Thermodynamic parameters for fluoride adsorption by PBA.

T(K)	ΔGº(kJ.mol^{-1})	ΔHº (kJ.mol^{-1})	ΔSº (kJ.mol^{-1}K^{-1})	Kc
293	-1.6506	-0.00392	0.00510	1.0006
303	-2.7374	-0.00737	0.00901	1.0011
323	-3.7936	-0.00778	0.01292	1.0016

The values of ΔH° and ΔS° can be obtained from the slope and intercept of a plot of ln(qe/ce) Vs 1/T as shown in Figure 14. The values of Kc, ΔG°, ΔH° and ΔS° are presented in Table 4. The negative ΔGº value confirmed the feasibility of the sorption process and the spontaneous nature of adsorption. The negative value of ΔHº obtained indicated the exothermic nature of the process. The positive ΔSº value indicated the affinity of the adsorbent for Fluoride removal.

Regeneration and Reuse: A fluoride adsorption experiment with initial concentration of 5mg l^{-1}, dose of 3g l^{-1} and contact time of 24hr was performed and the material was then separated by filtration and dried in an oven at 70^{o} C. This material was then used to perform the next adsorption experiment to determine its reusability as shown in Figure 15. It can be seen that after three cycles, the used adsorbent shows slightly less adsorption capacity than the second reuse material. The fluoride removal increases from 72.55, 97.05, and 98.84 % for fresh, first reuse, second reuse. The weight loss is 1.67 and 3.00% for first and second reuse cycle. After 3% weight loss of adsorbent, PBA might be available in the optimum dose for the initial fluoride concentration of 5mg L^{-1}. After second reuse, fluoride removal decreases from 98.84 to 92.55%, 92.55 to 74.07% and 74.07 to 54.24 % for third, fourth, and fifth reuses or regeneration cycle respectively (very high reuse capacity). Because of increasing weight loss from 4.67% to 10.67% PBA adsorbent shows a decrease in fluoride removal efficiency after a second reuse cycle. The weight loss can be controlled by preparing mechanically stable pellets of PBA sample. Thus, it is possible to regenerate this material by using commercially available alum. Further studies for optimization of the regeneration process are under progress. The reusability of the adsorbent was studied to check the residual fluoride uptake capacity. The reusability experiment was carried out by repeating the adsorption experiment on used and oven dried sample under the similar condition used for the first cycle shown in Figure 15. It was observed that the used adsorbent still have significant fluoride uptake capacity. Reuse study shows that up to 4th cycle material have fluoride removal efficiency more than 90% after that decreases to 54% due to its weight loss 10.67% repetition. This indicates that the adsorbent does not exhaust its fluoride uptake capacity in four cycles and oven drying of the used sample results in significant fluoride adsorption in subsequent cycles-. After complete saturation, the exhausted adsorbent was subjected to regeneration using different regeneration media. It was observed that multiple treatments with an alum solution appears to be the promising regeneration media and a maximum of 80% regeneration was achieved with alum.

Regeneration of spent alum: With an aim to address the problem of handling the spent regenerant (alum) and decreasing or using the quantity of fluorine-containing waste sludge the following new approaches are being pursued in our group to handle spent regenerant and reduce waste sludge as depicted in Figure 16.

It is reported that aluminium exhibits a higher bonding strength with fluorine compared with calcium. Aluminium can, therefore, remove fluorine in the waste water down to a lower concentration. However, the problems of aluminium are that aluminium is much more expensive than the calcium source, and sludge generated after treatment has a poor dehydrating capability. For these reasons, aluminium is inappropriate for high concentration fluoride treatment and, therefore, is mainly used for low concentration fluoride containing waste water. Taking these limitations into account, the two approaches pursued in our group appears to resolve the problems. The details are as follows:

Approach -I: In this method, a calcium source (slaked lime), which is generally inexpensive and abundantly available, is added to the aluminium fluoride complex generated after treating fluoride-containing adsorbent with alum. The aluminium of aluminium fluoride complex is was substituted with calcium. Aluminium in sludge dissolves, and is recovered and reused as a regenerant (alum). The CaF_4 so obtained is mixed with 3% chitosan solution to obtain CaF /chitosan composite. This composite was then tested for fluoride leaching, and negligible fluoride leaching was observed. The composite so obtained is a high value added product and can be used for shielding greenhouse from UV light.[27] Alternately CaF can be used in laser reflection lens made up of thin films with high refractive index and optical films with low refractive index alternately stacked on a quartz glass substrate. For an argon fluoride or a krypton fluoride excimer laser device, calcium fluoride (CaF_2) is commonly used as a coating material for the ultraviolet region. The recovered alum can be used for regeneration

$$2AlF_3 + 3Ca^{2+} \xrightarrow{NaOH} 3CaF_4 + 2AlO_2 + 4H^+ + 2Na^+$$

Approach-II: The regenerant (alum) bearing about 21mg/l fluoride (after repeated use) has been admixed with chitosan solution (chitosan dissolved in 3% acetic acid) in the ratio of 1:10.The composite so obtained has been tested for fluoride leaching. Negligible leaching of fluoride was observed on treating the composite with water for about 24 hours. The composite developed is transparent and may prove to be useful for optic applications. Aluminium fluoride (AlF_3) is a low-refractive-index material widely used in coatings for deep-ultraviolet (DUV) optical systems, especially 193 nm laser systems.[28] The proof of concept has been tested for above two approaches. The composite has been tested with negligible leaching of fluoride. These composite then have potential application as of the materials. The concept of simultaneous defluoridation and value is summarized in **Fig.17**. Further detailed studies are in progress to derive the mass and energy balance.

Scenario- I

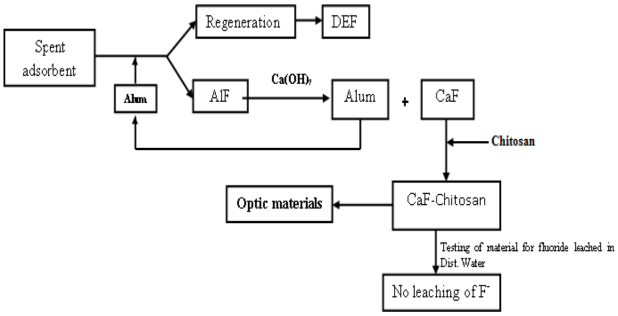

Safe handling of spent adsorbent and AlF complex

Scenario- II

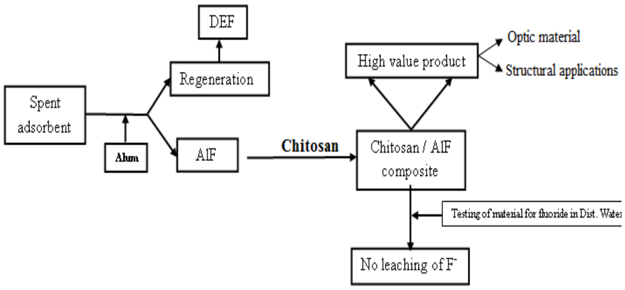

Safe handling of alum (regenerant)

Figure 16: The new approaches being pursued in our group to handle spent regenerant.

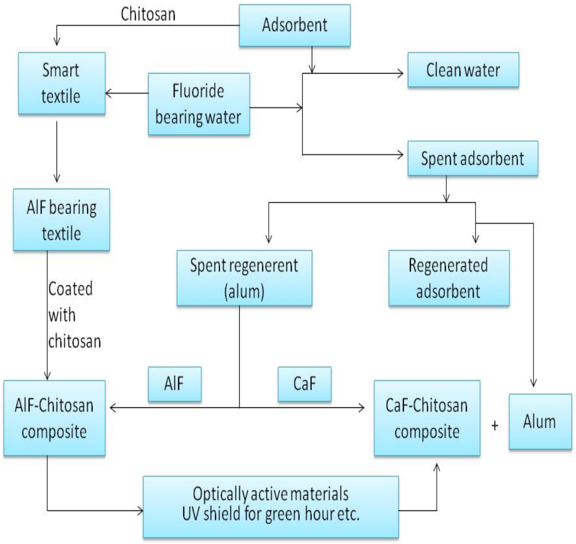

Figure17: Concept of simultaneous defluoridation.

Comparison with other adsorbents: The maximum fluoride adsorption capacity of PBA and other adsorbents has been listed in **Table 5**. According to the studies of the table it has been cleared that PBA is providing better adsorption capacities than other adsorbents. When the treatment characteristics of other adsorbents are compared with PBA, it is suggested that PBA is capable of effectively removing fluoride at a pH of 7. All such research studies conclude that PBA is a capable absorbent for the fluoride removal in drinking water.

CONCLUSION: *Polyalthia longifolia* (false Ashoka tree) leaf based alumina (PBA), a low cost composite adsorbent has been synthesized for removal of excess fluoride from drinking water with exceptionally good adsorption capacity of 17.57 mg g^{-1} at initial fluoride concentration of 5 mg l^{-1} using very low dose of 0.4 g l^{-1} as compared to 1.82 mg g^{-1} for activated alumina. The composite adsorbent has heterogeneous phases of $Al(OH)_3$ and Al_2O_3 encapsulated with carbon and $Al(OH)_3$ and Al_2O_3 deposited on carbon along with free $Al(OH)_3$ and alumina. Studies are now in progress for breakup synthesis to identify the phase showing a most extreme of fluoride removal. It was observed that numerous treatments with alum solution appear to recover the adsorbent to a maximum of 80% recovery. The adsorbent is performing quite well in the presence of other anions and henceforth can likewise be utilized for wastewater treatment.

Table 5: The comparison of maximum fluoride adsorption capacities of various adsorbents.

Adsorbent	$q_m\,(mg/g)$	References
Chitosan	1.39	29
siderite	1.60	30
GZI	9.80	31
Magnesia/chotisan composite	16.667	32
PBA	17.57	Present study

ACKNOWLEDGEMENT: A part of this work has been carried out under the CSIR-Network Project ESC-0306 & ESC-0108. The authors are grateful to the Director, CSIR-NEERI for providing research facilities.

REFERENCES:

1. Cengeloglu, Y., Kir, E., Ersoz, M., Buyukerkek, T., & Gezgin, S. (2003) Recovery and concentration of metals from red mud by donnan dialysis. *Colloid and Surfaces A: Physicochemical and Engineering Aspects*, 223 (1-3), 95-101. http://dx.doi.org/10.1016/j.chb.2008.02.012
2. Ali, I., Khan, T.A., & M. Asim, M. (2011) Removal of arsenic from water by electrocoagulation and electrodialysis techniques. *Separation & Purification Reviews*, 40 (1), 25-42. http://dx.doi.org/10.1080/15422119.2011.542738
3. Saleh, T.A., & Gupta, V.K. (2011) Functionalization of tungsten oxide into MWCNT and its application for sunlight-induced degradation of rhodamine, *Journal of Colloid and Interface Science*, 362 (2), 337-344. http://dx.doi.org/10.1016/j.jcis.2011.06.081
4. Saleh, T.A., Agarwal, S., & Gupta, V.K. (2011) Synthesis of MWCNT/MnO_2 and their application for simultaneous oxidation of arsenite and sorption of arsenate, *Applied Catalysis B: Environmental*, 106 (1-2),46-53. http://dx.doi.org/10.1016/j.apcatb.2011.05.003
5. Dantas, T.N.D.C., Neto, A.A.D., & Moura, M.C.P.D.A. (2001) Removal of chromium from aqueous solutions by diatomite treared with microemulsion, *Water Research*, 35 (9), 2219-2224. http://dx.doi.org/10.1016/S00431354(00)00507-8
6. Fu, F., & Wang, Q. (2011) Removal of heavy metal ions from wastewaters: A review, *Journal of Environmental Management*, 92 (3),407-418 http://dx.doi.org/10.1016/j.jenvman.2010.11.011
7. Daifullah, A.A.M., Yakout, S.M., & Elreefy, S.A. (2007) Adsorption of fluoride in aqueous solutins using $KMnO_4^-$ modified activated carbon derived from steam pyrolysis of rice straw, *Journal of Hazardous Materials*, 147 (1-2),633-643. http://dx.doi.org/10.1016/j.jhazmat.2007.01.062
8. Li, Y.-H., Wang, S., Zhang, X., Wei, J., Xu, C., Luan, Z., & Wu, D. (2003) Adsorption of fluoride from water by aligned carbon Nanotubes, *Materials Research Bulletin*, 38 (3), 469-476. http://dx.doi.org/10.1016/S0025-5408(02)01063-2
9. Tanna, A., Nair, R., & Chanda, S. (2009) Assessment of anti-inflammatory and hepatoprotective potency of polyalthia longifolia var pendula leaf in wister albino rats., *J. Nat. Med*, 63 (1), 80-85. http://dx.doi.org/10.1007/s11418-008-0288-2
10. Gupta, N., Kushwaha, A.K. & Chattopadhyaya, M. C. (2012) Adsorption studies of cationic dyes onto ashoka (saracaasoca) leaf powder. *Journal of the Taiwan Institute of Chemical Engineers*, 43 (4), 604-613. http://dx.doi.org/10.1016/j.jtice.2012.01.008
11. Lunge, S., Thakre, D., Kamble, S., Labhsetwar, N., & Rayalu, S. (2012) Alumina supported carbon composite material with exceptionally high defluoridation property from eggshell waste. Journal of Hazardous Materials, *J. Hazard. Mater*, 237-238, 161-169. http://dx.doi.org/10.1016/j.jhazmat.2012.08.023
12. Mohammad, F., Plessis, L., & Arfin, T. (2013) X-ray analysis of metal oxide-metal core-shell nanoparticles. In K. Shih, (Eds.), *X-Ray Diffraction: Structure, Principles and Applications*, (pp. 161-181). Nova Science Publishers, New York.
13. Prabhu, B., Suryanarayana, C., An, L. & Vidyanathan, R (2006) Synthesis and characterization of high volume fraction Al-Al_2O_3 nanocomposite powders by high-energy-milling, *Materials Science and Engineering: A*, 425 (1-2), 192-200. http://dx.doi.org/10.1016/j.msea.2006.03.066
14. Arfin, T., & Rafiuddin (2009) Transport studies of nickel arsenate membrane. *Journal of Electroanalytical Chemistry*, 636 (1-2), 113-122. http://dx.doi.org/10.1016/j.jelechem.2009.09.019
15. Arfin, T., Falch, A., & Kriek, R.J. (2012) Evaluation of charge density and the theory for calculating membrane potential for a nano-composite nylon-6,6 nickel phosphate membrane, *Physical Chemistry Chemical Physics*, 14 (48) 16760-16769. http://dx.doi.org/10.1039/c2cp42683h.
16. Wijna, H., & Schulthess, C.P. (2000) Vibrational spectroscopy study of selenite and sulphate adsorption mechanisms on Fe and Al (Hydroxide surfaces, *Journal of Colloid and Interface Science*, 229 (1), 286-297.

http://dx.doi.org/10.1006/jcis.2000.6960

17. Jagtap, S., Thakre, D., Wanjari, S., Kamble, S., Labhsetwar, N., & Rayalu, S. (2009) New modified chitosan-based adsorbent for defluoridation of water, *Journal of Colloid and Interface Science*, 332 (2) (2009) 280-290. http://dx.doi.org/10.1016/j.jcis.2008.11.080
18. Shi, Q., Huang, Y., & Jing, C. (2013) Synthesis, characterization and application of lanthanum-impregnated activated alumina for F removal, *Journal of Materials Chemistry A*, 1 (48), 12797-12803. http://dx.doi.org/10.1039/C3TA12548C
19. Yu, Y., & Chen, J.P. (2014) Fabrication and performance of a Mn-La metal composite for remarkable decontamination of fluoride, *Journal of Materials Chemistry A*, 2 (48) (20), 8086-8093. http://dx.doi.org/10.1039/C3TA15251K
20. Chen, L., Wang, T.-J., Wu, H.-X., Jin, Y., & Dou, X.-M. (2011) Optimization of a Fe-Al-Ce nano-adsorbent granulation process that used spray coating in a fluidized bed for fluoride removal from drinking water, *Powder Technology*, 206 (3), 291-296. http://dx.doi.org/10.1016/j.powtec.2010.09.033
21. Langmuir, I. (1916) The constitution and fundamental properties of solids and liquids. Journal of the American Chemical Society, *J. Am. Chem. Soc*, 38 (11) (1916) 2221-2295. http://dx.doi.org/10.1021/ja02268a002
22. Freundlich, H.M.F. (1906) Over the adsorption in solution. Journal of Phuysical Chemistry, 57, 385-470.
23. Sarkar, M., Banerjee, A., Pramanick, P.P. & Sarkar, A.R. (2006) Use of laterite for the removal of fluoride from contaminated drinking water, *Journal of Colloid and Interface Science*, 302 (2) (2006) 432-441. http://dx.doi.org/10.1016/j.jcis.2006.07.001
24. Wan, Z., Chen, W., Liu, C., & Dong, C. (2015) Preparation and characterization of γ-AlOOH@CS magnetic nanoparticle as a novel adsorbent for removing fluoride from drinking water, *Journal of Colloid and Interface Science*, 443,115-124. http://dx.doi.org/10.1016/j.jcis.2014.12.012
25. Weber, W.J. & Morris, J.C. (1963) Kinetics of adsorption on carbon from solution, *Journal of the Sanitary Engineering Division*, 89 (2), 31-60.
26. Dawood, S., & Sen, T. K. (2012) Removal of anionic dye Congo red from aqueous solution by raw pine and acid-treated pine cone powder as adsorbent: equilibrium, thermodynamic, kinetics, mechanism and process design, *Water Research, Water Res*, 46 (6) , 1933-1946. http://dx.doi.org/10.1016/j.watres.2012.01.009
27. Chu, C.W., Wei, C.T., Tsai, R.Y., & Ho, F.C. (2000) With low refractive index formed on a quartz glass substrate calcium fluoride (Caf2) and silicon dioxide (SiO2) mixed with a specific composition ratio; laser reflections lens; improved adhesion to the substrates, less porosity. US Patent, 6, 115179A.
28. Sun, J., Li, X., Zhang, W., Yi, K., & Shao, J. (2012) Effects of substrate temperatures and deposition rates on properties of aluminium fluoride thin films in deep-ultraviolet region, *Applied Optics*, 51 (35), 8481-8489. http://dx.doi.org/10.1364/AO.51.008481.
29. Sahli, M.A.M., Annouar, S., Tahaikt, M., Mountar, M., Soufiane, A., & Elmidaoui, A. (2007) Fluoride removal for underground brackish water by adsorption on the natural chitosan and by electrodialysis, *Desalination*, 212 (1-3) , 37-45. http://dx.doi.org/10.1016/j.desal.2006.09.018
30. Liu, Q., Guo, H., & Shan, Y. (2010) Adsorption of fluoride on synthetic siderite from aqueous solution, *J. Fluorine Chem*, 131 (5), 635-641. http://dx.doi.org/10.1016/j.jfluchem.2010.02.006
31. Dou, X., Zhang, Y., Wang, H., Wang, T., & Wang, Y. (2011) Performance of granular zirconium-iron oxide in the removal of fluoride from drinking water, *Water Research* 45 (12) , 3571-3578. http://dx.doi.org/10.1016/j.watres.2011.04.002
32. C.S. Sundaram, N. Viswanathan, S. Meenakshi, Defluoridation of water using magnesia/chotisan composite, *Journal of Hazardous Materials*, 163 (2-3), 618-624. http://dx.doi.org/10.1016/j.jhazmat.2008.07.009.